Deflection Adaptive LPV Control of an Active Suspension System

Oliver Fritsch, Guido Koch and Boris Lohmann

Abstract— **The conflict in the design of automobile suspension systems between ride-comfort, safe driveability in the sense of low dynamic wheel loads and limited suspension deflection can be eased by active suspensions. The versatility and performance of an active suspension system is further increased if its controller parametrization is adapted to the current driving state. This can be achieved by interpreting the parameter of a linear parameter varying (LPV) controller as a scheduling variable.**

In this paper an LPV controller is synthesized that establishes quadratic $\mathscr{H}_\infty$-performance γ of the generalized plant. Smooth scheduling between two controller settings is performed depending on the output of an adaptation logic that processes the suspension deflection signal. The intention is to design a comfort maximizing controller, which also satisfies safety and suspension stroke constraints. The focus is on preventing excessive suspension deflections for low-frequency road excitations, which are a problem for most conventional ride comfort oriented controllers if real measured road profiles are used as excitation.

I. Introduction

On the one hand side vehicle suspension systems should provide maximum passenger comfort on the other hand the vehicle is expected to be safely driveable, i.e to guarantee tire road contact. Furthermore the constraint of limited deflection of the primary spring needs to be considered for suspension design. These three requirements are conflicting due to the mechanical structure of the suspension system, [MW04]. However, the conflict can be eased by integrating controlled active or semiactive components in the suspension system.

In the controller design for active suspension systems it is desirable not to limit the flexibility of the systems by using a conservative, time-invariant control law. Some nonlinear approaches use switching controller structures which schedule between different controller settings based on certain scheduling parameters (e.g. dynamic wheel load or suspension deflection) and are well suited for suspension controller design ([LK97], [KDL08]). In this context also LPV methodologies are applied either to establish robustness against nonlinearities in an otherwise semiactive adaptive design ([ZSG$^+$08]) or to directly influence controller adaptation by using the parameter as a scheduling variable ([FB00], [FB02], [PVDS$^+$08]).

The controller design in this paper pursues the latter LPV approach, which uses weighting filters to shape the adaptive closed loop behavior of the system like in the common weighted $\mathscr{H}_\infty$-performance problem, [ZDG96]. In addition to generally increasing the comfort and keeping safety and maximum deflection constraints excessive suspension strokes should be suppressed for low-frequency road excitations. This has proven to be necessary in simulations using measurement data of real road profiles, since especially comfort oriented controllers tend to high suspension deflections for low-frequency excitations. The approach is to combine the good low-frequency performance ($< 0.7\,\mathrm{Hz}$) of a passive suspension with the superb performance of a comfort oriented active suspension for higher frequencies. This is achieved by smooth scheduling between two constituent controllers carried out by an adaptation logic depending on the frequency content of the measured suspension deflection signal. Since we use the polytopic LPV techniques described in [AGB95] for our design, stability and performance are guaranteed for arbitrary variations of the scheduling variable.

The paper is organized as follows: In Section II the model of the active suspension is given using the classical quarter car approach. Based on the explicitly given conflicting requirements in Section II, the synthesis of the adaptive LPV controller is presented in Section III. Section IV demonstrates the controller performance in simulations using real measured road profiles as excitation. Finally, a conclusion is given in Section V.

II. Modelling and System requirements

A. Suspension Model

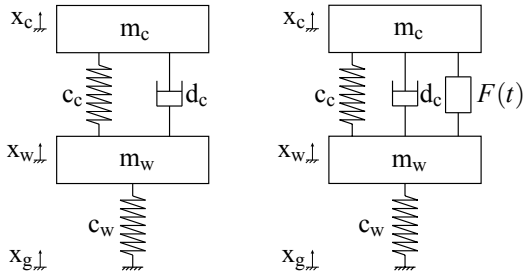

Fig. 1. Quarter car suspension models: Passive suspension (left) and high bandwidth active suspension (right)

If only the lift movement of a vehicle suspension is of interest, the well-known quarter car model can be used, which is illustrated in Figure 1, [MW04]. In this work, we consider a high bandwidth active suspension system, i.e. the actuator is integrated in parallel to the primary spring of the passive suspension system. The resulting control input is the actuator force $u(t) = F(t)$. If we define x_s to be the suspension deflection $x_s = x_c - x_w$, the considered output variables of the system are

$$\mathbf{y} = \left[\ \ddot{x}_c\ ,\quad \ddot{x}_w\ ,\quad x_s\ \right]^T, \tag{1}$$

All Authors are with the Institute of Automatic Control, Technische Universität München, 85748 Garching near Munich, Germany oliver.fritsch@tum.de, guido.koch@tum.de, lohmann@tum.de

ISBN 978-963-311-369-1

which reflects a realistic assumption for the available sensor combination used in modern upperclass vehicles. However, the measured output variables are assumed to be corrupted by measurement noise given by the vector $\mathbf{r} = \left[\; r_{\ddot{x}_c} \;,\quad r_{\ddot{x}_w} \;,\quad r_{x_s} \;\right]^T$. The dynamic wheel load, which can endanger tire road contact, is defined as

$$F_{\text{dyn}} = c_w\,(x_g - x_w)\;. \tag{2}$$

The main disturbance of the system is the vertical road displacement x_g such that the vector of disturbance inputs can be expressed as

$$\mathbf{w} = \left[\; x_g \;,\quad \mathbf{r}^T \;\right]^T\;. \tag{3}$$

The statevector of the fourth order model is

$$\mathbf{x} = \left[\; x_c \;,\quad \dot{x}_c \;,\quad x_w \;,\quad \dot{x}_w \;\right]^T\;. \tag{4}$$

Linear component characteristics assumed the following state space representation of the active suspension system results

$$\underbrace{\begin{bmatrix}\dot{x}_c\\ \ddot{x}_c\\ \dot{x}_w\\ \ddot{x}_w\end{bmatrix}}_{\dot{\mathbf{x}}} = \underbrace{\begin{bmatrix}0 & 1 & 0 & 0\\ -\frac{c_c}{m_c} & -\frac{d_c}{m_c} & \frac{c_c}{m_c} & \frac{d_c}{m_c}\\ 0 & 0 & 0 & 1\\ \frac{c_c}{m_w} & \frac{d_c}{m_w} & -\frac{c_c+c_w}{m_w} & -\frac{d_c}{m_w}\end{bmatrix}}_{\mathbf{A}_{\text{susp}}}\underbrace{\begin{bmatrix}x_c\\ \dot{x}_c\\ x_w\\ \dot{x}_w\end{bmatrix}}_{\mathbf{x}} + \underbrace{\begin{bmatrix}0 & 0 & 0 & 0\\ 0 & 0 & 0 & 0\\ 0 & 0 & 0 & 0\\ \frac{c_w}{m_w} & 0 & 0 & 0\end{bmatrix}}_{\mathbf{B}_{1,\text{susp}}}\underbrace{\begin{bmatrix}x_g\\ r_{\ddot{x}_c}\\ r_{\ddot{x}_w}\\ r_{x_s}\end{bmatrix}}_{\mathbf{w}} + \underbrace{\begin{bmatrix}0\\ \frac{1}{m_c}\\ 0\\ -\frac{1}{m_w}\end{bmatrix}}_{\mathbf{b}_{2,\text{susp}}}\underbrace{F}_{u}, \tag{5}$$

$$\underbrace{\begin{bmatrix}\ddot{x}_c\\ \ddot{x}_w\\ x_s\end{bmatrix}}_{\mathbf{y}} = \underbrace{\begin{bmatrix}-\frac{c_c}{m_c} & -\frac{d_c}{m_c} & \frac{c_c}{m_c} & \frac{d_c}{m_c}\\ \frac{c_c}{m_w} & \frac{d_c}{m_w} & -\frac{c_c+c_w}{m_w} & -\frac{d_c}{m_w}\\ 1 & 0 & -1 & 0\end{bmatrix}}_{\mathbf{C}_{2,\text{susp}}}\mathbf{x} + \underbrace{\begin{bmatrix}0 & 0 & 0 & 0\\ \frac{c_w}{m_w} & 0 & 0 & 0\\ 0 & 0 & 0 & 0\end{bmatrix}}_{\mathbf{D}_{21,\text{susp}}}\mathbf{w} + \underbrace{\begin{bmatrix}\frac{1}{m_c}\\ -\frac{1}{m_w}\\ 0\end{bmatrix}}_{\mathbf{d}_{22,\text{susp}}}u\;. \tag{6}$$

The measured signals are

$$\underbrace{\begin{bmatrix}\ddot{x}_{cm}\\ \ddot{x}_{wm}\\ x_{sm}\end{bmatrix}}_{\mathbf{y}_m} = \mathbf{C}_{2,\text{susp}}\mathbf{x} + \underbrace{\begin{bmatrix}0 & 1 & 0 & 0\\ \frac{c_w}{m_w} & 0 & 1 & 0\\ 0 & 0 & 0 & 1\end{bmatrix}}_{\mathbf{D}_{21m}}\mathbf{w} + \mathbf{d}_{22,\text{susp}}u\;. \tag{7}$$

The vector $\mathbf{e}$ defined as

$$\mathbf{e} = \begin{bmatrix}\ddot{x}_c\\ F\end{bmatrix} = \underbrace{\begin{bmatrix}-\frac{c_c}{m_c} & -\frac{d_c}{m_c} & \frac{c_c}{m_c} & \frac{d_c}{m_c}\\ 0 & 0 & 0 & 0\end{bmatrix}}_{\mathbf{C}_{1,\text{susp}}}\mathbf{x} + \underbrace{\begin{bmatrix}\frac{1}{m_c}\\ 1\end{bmatrix}}_{\mathbf{d}_{12,\text{susp}}}u \tag{8}$$

contains the so called error signals which are minimized by the LPV weighted $\mathscr{H}_\infty$-controller presented in Section III. The parameters used in the model are given in Table I.

TABLE I
SUSPENSION PARAMETERS

Parameter	Symbol	Value	Unit
Chassis mass	m_c	256	[kg]
Unsprung mass	m_w	31	[kg]
Primary spring stiffness	c_c	20200	[N/m]
Tire stiffness	c_w	128000	[N/m]
Chassis damping ratio	d_c	1140	[Ns/m]
Resonance frequency chassis	$f_c = \frac{1}{2\pi}\sqrt{\frac{c_c}{m_c}}$	1.41	[Hz]
Resonance frequency wheel	$f_w = \frac{1}{2\pi}\sqrt{\frac{c_c+c_w}{m_w}}$	11.00	[Hz]

B. System requirements

The primary objective of the active suspension system is to maximize ride comfort, which can be mathematically formulated as the minimization of the RMS-value $\|\cdot\|_{\text{rms}}$ of vertical chassis acceleration

$$\min\left(\|\ddot{x}_c\|_{\text{rms}}\right)\;. \tag{9}$$

A measure for ride safety is the dynamic wheel load. To prevent the tire from loosing the road contact it should not fall below the negative value of the static wheel load

$$\min(F_{dyn}) \geq -F_{\text{stat}} = -2815.47\,\text{N}\;. \tag{10}$$

Its RMS-value should be bounded by

$$\|F_{dyn}\|_{\text{rms}} \leq \frac{F_{\text{stat}}}{3} = 938.49\,\text{N}\;. \tag{11}$$

This RMS-bound for the wheel load can be derived if the disturbance signal is assumed to be Gaussian white noise using the 3σ-rule (see e.g. [WPO95]) and it guarantees that in 99.7% of the time the magnitude of the dynamic wheel load does not exceed the static wheel load thus preserving tire road contact.

The absolute construction-conditioned limits for the deflection of the primary spring are assumed to be

$$\max\left(|x_s|\right) \leq x_{s\max} = 0.1\,\text{m}\;. \tag{12}$$

By applying the 3σ-rule again it is derived that the RMS-value of the suspension deflection should not exceed

$$\|x_s\|_{\text{rms}} \leq \frac{x_{s\max}}{3} = 0.033\,\text{m}\;. \tag{13}$$

The maximum peak force of the actuator and its admissible RMS force value result in the constraints

$$\max\left(|F|\right) \leq F_{\max} \;=\; 4000\,\text{N}\;, \tag{14}$$

$$\|F\|_{\text{rms}} \;\leq\; 800\,\text{N}\;. \tag{15}$$

The actuator bandwidth limitation is assumed to be fulfilled if 99% of the actuator's power is allocated in the frequency range from 0 Hz to 10 Hz. This can be expressed using the one sided spectral density $S_F(f)$ to obtain the power ratio V_{10} as

$$V_{10} = \frac{\int_0^{10} S_F(f)\,df}{\int_0^{\infty} S_F(f)\,df} \geq V_{10\,\min} = 0.99\;. \tag{16}$$

The force and bandwidth constraints of the actuator correspond to an electrical linear motor used in a quarter-vehicle test-setup at the authors' institute.

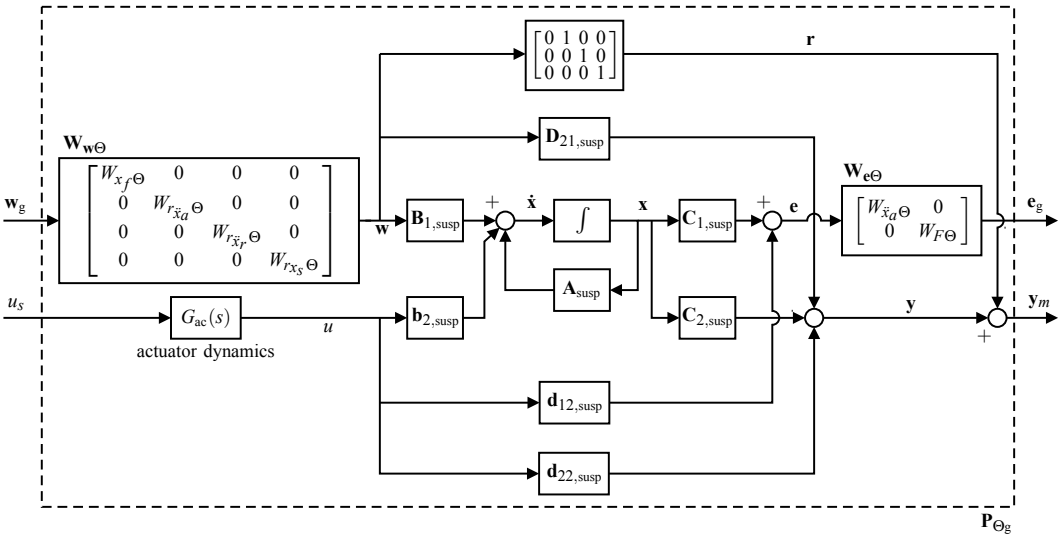

Fig. 2. Generalized plant $\mathbf{P}_{\Theta_g}$ of the active suspension system

III. Controller Synthesis

A. Adaptive $\mathscr{H}_\infty$-control

In [Bec93] the common suboptimal $\mathscr{H}_\infty$-control problem (see e.g. [ZDG96]) is generalized to LPV plants controlled by LPV controllers. It is shown that under certain conditions the existence of a solution to a given LMI system (usually infinite dimensional) guarantees the existence of an LPV controller which provides stability by a common quadratic Lyapunov function and a limitation of the induced $\mathscr{L}_2$-norm by a known scalar γ for arbitrary parameter variations. In [AGB95] the expression *quadratic $\mathscr{H}_\infty$-performance γ* is introduced for LPV systems with these properties. Based on a solution of the LMI system such a controller can be computed. Since we want to design an adaptive active suspension controller, the LPV formalism is appropriate for our problem description if we interpret the system parameter θ as a scheduling variable. By augmenting our LTI plant with parameter dependent LPV weighting filters $\mathbf{W}_{\mathbf{w}\Theta}$ and $\mathbf{W}_{\mathbf{e}\Theta}$ (see Figure 2) we can formulate our design task as an LPV version of a weighted $\mathscr{H}_\infty$-performance problem. Hence the controller design methods of [Bec93] are applicable to the generalized plant $\mathbf{P}_{\Theta_g}$ in Figure 2. In general the parameter θ could be vector valued but in this paper we will examine the scalar case meaning $\theta \in \Theta$ where Θ is a closed interval $\Theta \subset \mathbb{R}$. The generalized plant can be described by

$$\mathbf{P}_{\Theta_g} = \begin{cases} \dot{\mathbf{x}}_g = \mathbf{A}_g(\theta)\mathbf{x}_g + \mathbf{B}_{1_g}(\theta)\mathbf{w}_g + \mathbf{b}_{2_g}(\theta)u \\ \mathbf{e}_g = \mathbf{C}_{1_g}(\theta)\mathbf{x}_g + \mathbf{d}_{12_g}(\theta)u \\ \mathbf{y}_m = \mathbf{C}_{2_g}(\theta)\mathbf{x}_g + \mathbf{D}_{21_g}(\theta)\mathbf{w}_g + \mathbf{d}_{22_g}u \end{cases} \tag{17}$$

and an appropriate controller is of the form

$$\mathbf{K}_\Theta = \begin{cases} \dot{\mathbf{x}}_K = \mathbf{A}_K(\theta)\mathbf{x}_K + \mathbf{B}_K(\theta)\mathbf{y} \\ u = \mathbf{C}_K(\theta)\mathbf{x}_K + \mathbf{D}_K(\theta)\mathbf{y}\,. \end{cases} \tag{18}$$

B. Performance considerations and special cases

Usually the LMI system given in [Bec93] is of infinite dimension since it has to be solved for every admissible θ. Therefore to applicate the design method in practice the parameter space has to be gridded and the LMI system is only solved at the grid points. By this dilution of the original LMI constraint, quadratic $\mathscr{H}_\infty$-performance γ cannot be guaranteed anymore for arbitrary variations of the parameter θ. Adaptive LPV suspension controllers as suggested by other authors e.g. Fialho and Balas [FB00] suffer from this fact. However as already mentioned in [Bec93] there exist special cases in which the LMI system reduces to finite dimensions although quadratic $\mathscr{H}_\infty$-performance γ is still guaranteed for the closed loop system. These special cases are discussed in [AGB95] and presume certain features of the plant and the parameter space. The additional requirements are:

- **(A1)** The LPV plant is polytopic as defined in [AGB95].
- **(A2)** $\mathbf{D}_{22} = \mathbf{0}$ and $\mathbf{B}_2$, $\mathbf{C}_2$, $\mathbf{D}_{12}$, $\mathbf{D}_{21} = \text{const.}$ for all θ in the polytopic parameter space Θ.

If these requirements are fulfilled it is sufficient to solve all LMIs involved in the controller design process suggested in [AGB95] only at the vertices of the parameter polytope Θ. Since we formulate our control problem such that **(A1)** and **(A2)** hold for the generalized plant we use these methods to find an LPV controller guaranteeing stability and minimizing γ.

C. Design of the weighting filters

As in the common weighted $\mathscr{H}_\infty$-performance problem (see e.g. [ZDG96]) the weighting filters are the design parameters of the controller synthesis. For the weights of the disturbances summarized in $\mathbf{W}_{\mathbf{w}\Theta}$ we choose constants approximately characterizing the noise intensity of the different disturbance sources. The weight for the road disturbance is $W_{x_f\Theta} = 0.01$ and those characterizing the sensor noise are $W_{r_{\ddot{x}_w}\Theta} = W_{r_{\ddot{x}_c}\Theta} = \sqrt{1.10 \cdot 10^{-8}}$ and $W_{r_{x_s}\Theta} = \sqrt{1.95 \cdot 10^{-11}}$. The adaptive behavior of the controller is enforced by a parameter dependent choice of the error weights summarized in $\mathbf{W}_{\mathbf{e}\Theta}$. Our intention is to design a controller which focuses

on ride comfort whenever possible and which becomes increasingly inactive when low-frequency road disturbances are dominant. Thus we avoid critically high suspension deflections by exploiting the good low-frequency behavior (below approx. 0.7 Hz) of the passive system. We specify that our scheduling variable θ ranges within the interval $\Theta = [0, 1]$ and we choose

$$W_{\ddot{x}_a\Theta}(s) = \frac{30}{\frac{1}{0.15}s+1} + \theta \cdot \frac{-19}{\frac{1}{0.15}s+1} \tag{19}$$

and

$$W_{F\Theta}(s) = \frac{1.0\cdot 10^{-3}\cdot(\frac{1}{50}s+1)}{\frac{1}{500}s+1} + \theta \cdot \frac{3.4\cdot 10^{-3}\cdot(\frac{1}{50}s+1)}{\frac{1}{500}s+1}. \tag{20}$$

Clearly this frequency domain representation of the LPV weights is only valid for constant values of θ, but this form shows the influence of the parameter best. As one can see in (19) and (20) the gains of the filters change along with the scheduling variable θ. For $\theta = 0$ the gain of $W_{\ddot{x}_a\Theta}(s)$ is high, enforcing a reduction of the body acceleration and simultaneously the gain of $W_{F\Theta}(s)$ is low, allowing high actuator activity. When θ approaches one the gain of $W_{\ddot{x}_a\Theta}(s)$ is decreasing and that of $W_{F\Theta}(s)$ is increasing. Hence the actuator activity is penalized heavily and the controller becomes increasingly inactive. By choosing polytopic state space realizations based on the controllable canonical form for (19) and (20) and by introducing an actuator model

$$G_{\text{ac}}(s) = \frac{1}{\frac{1}{2\pi\cdot 100}s+1} \tag{21}$$

we can ensure that **(A1)** and **(A2)** are satisfied for the generalized plant (17). Note that the actuator model (21) has a very high cut-off frequency at 100 Hz and hence does not alter the original problem significantly. However our simulation results show that the essential part of the actuator activity takes place in the frequency range below 10 Hz and the constraint formulated in (16) is clearly met.

Figure 3 shows Bode plots of the resulting LPV controller for constant values of θ at the vertices of the parameter space Θ compared to those of the passive suspension. The similarity between the passive and the active suspension for $\theta = 1$ is obvious. For the vertex $\theta = 0$ the active system exhibits considerable advantages over the passive one in the region of the chassis resonance frequency. Note that this is also true for the suspension and tire deflection even though they were not included in the weighting process. Only in the low-frequency range the controller for this vertex leads to significantly higher gains for the suspension deflection compared to the passive system (see Figure 3a)).

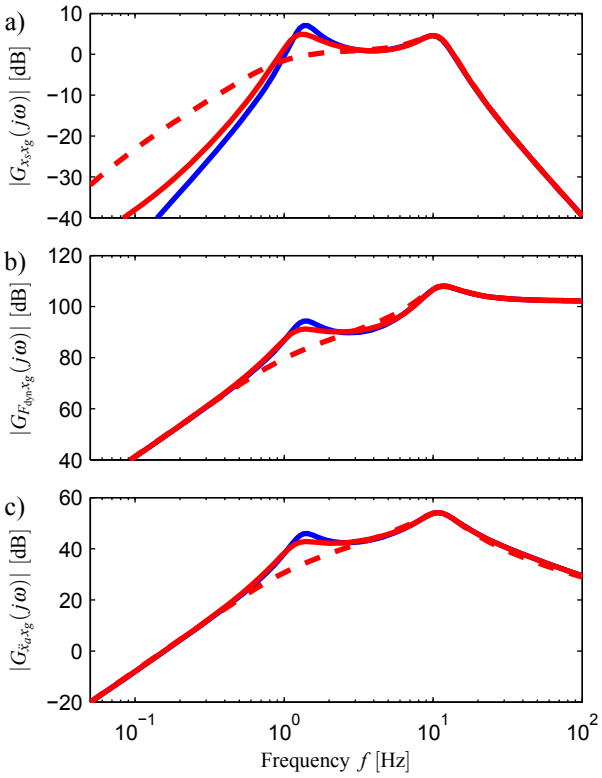

Fig. 3. Bode plots of the passive suspension (blue) and the LPV controlled suspension system at the vertices of the parameter space. Vertex $\theta = 0$ (red, dashed) and vertex $\theta = 1$ (red, solid). Amplitude-frequency response a) from x_g to x_s, b) from x_g to F_{dyn}, c) from x_g to $\ddot{x}_c$.

D. Controller Adaptation

After the synthesis of the parameter dependent controller an adaptation logic (see Figure 4) is designed for the scheduling task. The controller behavior shall change with the intensity of the road excitation in the low-frequency range. Considering the measurement signals (7) and the frequency response in Figure 3a) this quantity is best reflected in the suspension deflection x_s. Hence we use this signal as the input for the adaptation logic. To focus only on the low-frequency part of the signal it is filtered first by a second order low-pass with a cut-off frequency at 0.64 Hz. A measure for the energy contained in the resulting signal $\tilde{x}_s$ is its RMS-value, which is estimated using a procedure described e.g. in [Ven93]. The signal is squared and once more low-pass filtered. The resulting quantity p is then compared to an empirically determined constant, which represents an energy level that can be tolerated without adapting the controller. Lower values of p initiate an adaptation towards ride comfort whereas higher values shift the focus on suppressing low-frequency suspension deflections. This is achieved by multiplying the difference D by a constant and subsequent integration with saturation limits at zero and one. The output of the adaptation logic is the scheduling variable θ.

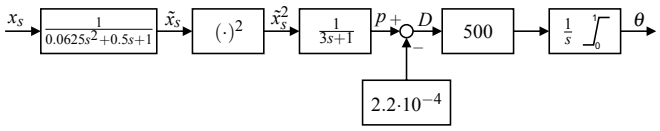

Fig. 4. Adaptation logic

IV. Simulation Results

In order to evaluate the performance of the LPV controller it has been tested in simulation using two concatenated measured road profiles as excitation. The vehicle drives over the resulting road profile with a given velocity trajectory displayed in Figure 5a) (scaled by a factor of 0.03 for visualization purposes). The corresponding road excitation signal is already given as a function of time in Figure 5a). The first profile originates from a highway and contains mainly low-frequency excitation and the second profile relates to a test-track with two bumps and primarily high-frequency excitation. Note that the magnitude of the road irregularities is up to 2 m and the broadband nature of the excitation signal is not well reflected in Figure 5a) due to the scaling.

The measurement disturbances are incorporated into the simulation as band-limited white noise with a bandwidth of 1 kHz. Within this frequency range the one sided power spectral density exhibits a constant value of $3.9 \cdot 10^{-11}\,\mathrm{m^2 s}$ for the suspension deflection measurement noise r_{x_s} and $2.5 \cdot 10^{-8}\,\frac{\mathrm{m^2}}{\mathrm{s^3}}$ for the noise signals $r_{\ddot{x}_c}$ and $r_{\ddot{x}_w}$.

In Figure 5 the trajectories of the relevant output variables are displayed for the active and the passive suspension as well as the scheduling parameter θ and the control force F in the active case. Moreover, the power spectral density of $\ddot{x}_c$ is shown in the frequency range below 3 Hz in Figure 5i).

Due to the high energy content of the suspension deflection signal in the low-frequency range the parameter θ rises during the first track section. This prevents the active suspension from hitting the limits. In the second section of the track the passive suspension violates the deflection constraint (compare Figures 5c) and d) at approx. 43sec and 49sec) while the active suspension still keeps the limits. The dynamic wheel load is reduced in the active case as well and - unlike the passive suspension - does not fall below the safety critical limit $-F_{\mathrm{stat}} = -2815.47\,\mathrm{N}$. Ride comfort is significantly increased by the minimization of vertical chassis acceleration, which can especially be seen in the second part of the road profile. Figure 5i) shows the power spectral density of $\ddot{x}_c$ for the road segments separately as well as for the complete track and highlights the significant comfort increase of the LPV controlled suspension. The control force is within the specified bounds of the considered actuator with an RMS-level of 280.63N, a peak value of 1365.96N and a power ratio $V_{10} = 0.9998$.

The performance benefit of the active suspension is summarized in Table II as the ratio between the relevant RMS-values of the active and the passive suspension. Regarding ride comfort and safety the performance of the active system is superior to the passive one including a comfort improvement of up to 43% on the second part of the road profile. The higher suspension deflection values of the active setting ($\|x_s\|_{\mathrm{rms}} = 0.0211\,\mathrm{m}$ and $\max(|x_s|) = 0.0773\,\mathrm{m}$) are no disadvantage since they are well below the tolerable maximum values specified in (12) and (13). Additionally a reproduction of the LPV controller described in [FB00] has been compared to our design using the same excitation signal. Its performance did not match our results in any of the control objectives. However the suspension deflection limit in [FB00] was assumed to be $\pm 0.08\,\mathrm{m}$ instead of 0.1 m, resulting unavoidably in a more conservative design.

TABLE II
RMS ratios of the active and passive suspension system

	$\frac{\|x_s\|_{\mathrm{rms}}}{\|x_{s,\mathrm{pas}}\|_{\mathrm{rms}}}$	$\frac{\|F_{\mathrm{dyn}}\|_{\mathrm{rms}}}{\|F_{\mathrm{dyn,pas}}\|_{\mathrm{rms}}}$	$\frac{\|\ddot{x}_c\|_{\mathrm{rms}}}{\|\ddot{x}_{c,\mathrm{pas}}\|_{\mathrm{rms}}}$
First road section	1.356	0.985	0.926
Second road section	0.804	0.689	0.574
Complete road profile	1.021	0.886	0.743

V. Conclusion and Outlook

An adaptive LPV controller has been designed that interpolates smoothly between two controller settings depending on the frequency content of the suspension deflection signal. The design uses some exceptional features like the polytopic properties of the generalized plant and the chosen scheduling parameter space to ensure stability and performance of the closed loop system already in the design process. The controller has been tested using measured data of real road profiles and the active suspension gives superior performance compared to the passive suspension system resulting in a comfort increase of up to 43% in terms of the RMS-value of vertical chassis acceleration. Every constraint formulated in Section II-B is kept by the LPV controlled active suspension.

The next research step will be to test the controller performance at a quarter-vehicle test-rig.

References

[AGB95] P. Apkarian, P. Gahinet, and G. Becker. Self-scheduled $\mathscr{H}_\infty$ control of linear parameter-varying systems: a design example. *Automatica*, 31(9):1251–1261, 1995.

[Bec93] G. Becker. *Quadratic Stability and Performance of Linear Parameter Dependent Systems*. PhD thesis, University of California at Berkley, 1993.

[FB00] I. J Fialho and G. J. Balas. Design of nonlinear controllers for active vehicle suspensions using parameter-varying control synthesis. *Veh. Syst. Dyn.*, 33:351–370, 2000.

[FB02] I. Fialho and G. J. Balas. Road adaptive active suspension design using linear parameter-varying gain-scheduling. *IEEE Trans. Contr. Syst. Tech.*, 10(1):43–54, 2002.

[KDL08] G. Koch, K. J. Diepold, and B. Lohmann. Multi-objective road adaptive control of an active suspension system. In *Motion and Vibration Control - Selected papers from MOVIC 2008*. Springer, 2008.

[LK97] J. Lin and I. Kanellakopoulos. Nonlinear design of active suspensions. *IEEE Contr. Syst. Mag.*, 17:45–59, 1997.

[MW04] M. Mitschke and H. Wallentowitz. *Dynamik der Kraftfahrzeuge*. Springer, Berlin, 2004.

[PVDS+08] C. Poussot-Vassal, A. Drivet, O. Sename, L. Dugard, and R. Ramirez-Mendoza. A self tuning suspension controller for multi-body quarter vehicle model. In *Proc. 17th IFAC World Congress*, 2008.

[Ven93] P. Venhovens. *Optimal Control of Vehicle Suspensions*. PhD thesis, Delft University of Technologie, 1993.

[WPO95] P. H. Wirsching, T. L. Paez, and K. Ortiz. *Random Vibrations – Theory and Practice*. John Wiley, New York, 1995.

[ZDG96] K. Zhou, J. Doyle, and K. Glover. *Robust and Optimal Control*. Prentice Hall, Upper Saddle River, New Jersey, 1996.

[ZSG+08] A. Zin, O. Sename, P. Gaspar, L. Dugard, and J. Bokor. Robust LPV-$\mathscr{H}_\infty$ control for active suspensions with performance adaptation in view of global chassis control. *Veh. Syst. Dyn.*, 46(10):889–912, 2008.

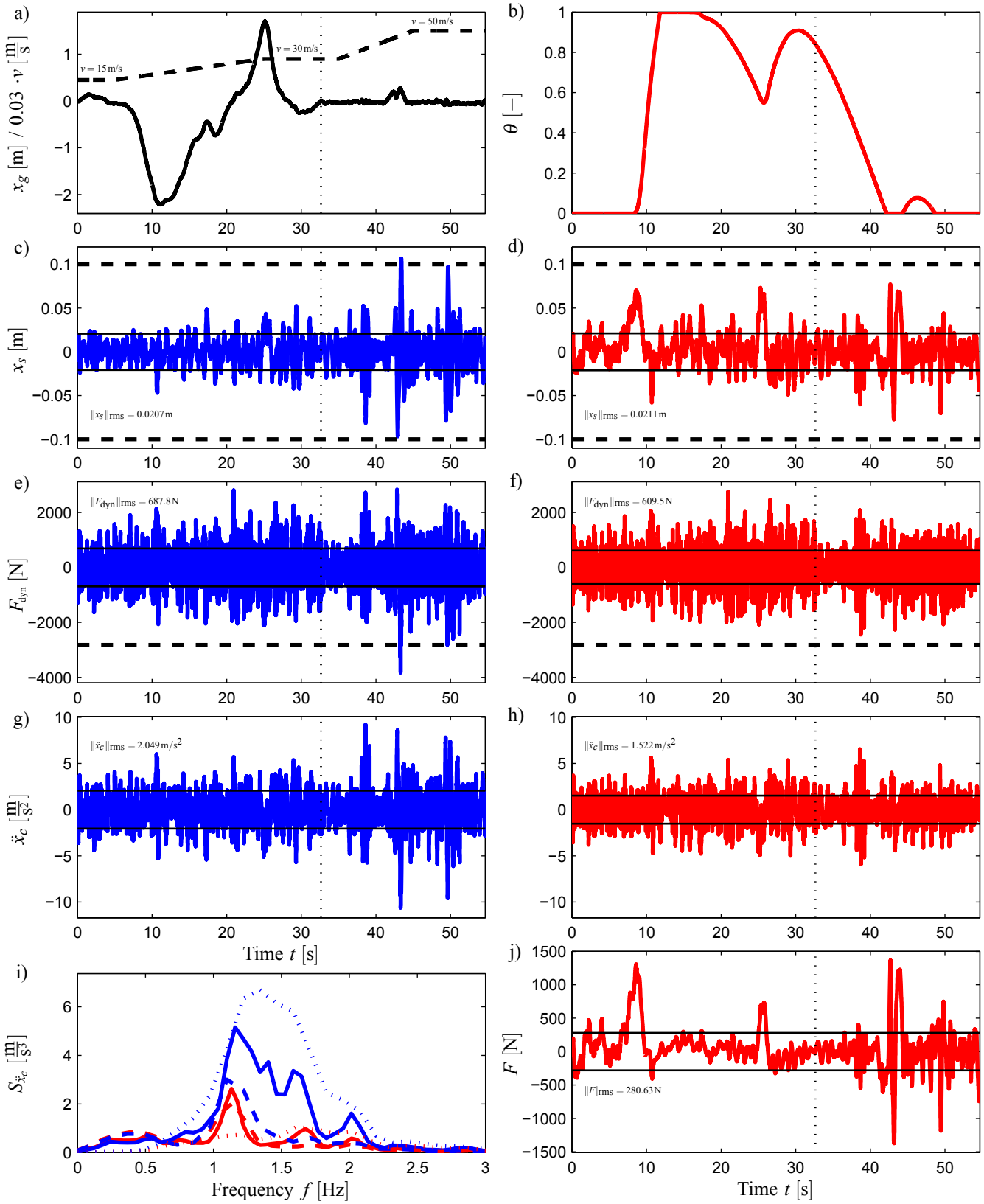

Fig. 5. Performance comparison of the passive and the active LPV controlled suspension system. a) Road excitation (solid) and scaled speed profile (dashed). Separation of the two characteristic road sections (black, dotted). b), c), d), e), f), g), h), j) Simulation results of relevant variables. Passive system (blue) and active system (red). Standard deviation given by the RMS-values (black, solid) and maximum tolerable values (black, dashed). Separation of the two characteristic road sections (black, dotted). i) One sided power spectral densities of the body acceleration. Passive system (blue) and active system (red). Complete road profile (solid), first section of the profile (dashed) and second section of the profile (dotted).